Research Paper

Imaging mass spectrometry reveals sodium lauryl sulfate-induced changes in skin lipoquality, principally affecting sphingomyelin

Yusuke Saito[1,2], Fumihiro Eto[1,2], Shiro Takei[1,2,3], Ikuko Yao[2,4]*, Mitsutoshi Setou[1,4]

[1] Department of Cell Biology and Anatomy, Hamamatsu University School of Medicine, 1−20−1 Handayama, Higashi-ku, Hamamatsu, Shizuoka 431−3192, Japan
[2] Department of Optical Imaging, Institute for Medical Photonics Research, Preeminent Medical Photonics Education & Research Center, Hamamatsu University School of Medicine, 1−20−1 Handayama, Higashi-ku, Hamamatsu, Shizuoka 431−3192, Japan
[3] Laboratory of Fish Biology, Department of Environmental Biology, College of Bioscience and Biotechnology, Chubu University, 1200 Matsumoto-cho, Kasugai, Aichi 487−8501, Japan
[4] International Mass Imaging Center, Hamamatsu University School of Medicine, 1−20−1 Handayama, Higashi-ku, Hamamatsu, Shizuoka 431−3192, Japan

Abstract Lipids and lipoqualities are important for skin barrier function. In previous reports, repeated irritation by sodium lauryl sulfate (SLS) was found to reduce epidermal barrier function and epidermal water content. Imaging mass spectrometry (IMS) can reveal not only the identity and localization of lipids in organs but also the distribution of administered drugs. Here, we attempted to visualize the distribution of SLS and changes in lipid composition in the epidermis of the skin. Initially, we histologically examined micro damage of the skin using trypan blue in the foot-pad of mice treated with SLS. Subsequently, we assessed the invasion of SLS and the effect of SLS on the lipid composition of the skin using IMS. We found that, relative to the foot-pad of mice treated with saline, the foot-pad of mice treated with SLS exhibited a significant change in *m/z* 817.71 associated with sphingomyelin despite the fact that no noticeable damage was observed in the layer structure dyed with trypan blue. Furthermore, we proved the penetration of SLS to the epidermis and dermis. The results suggest that SLS penetrates the skin tissue and alters the lipid composition on the skin surface.

Key words: Skin, Pharmaceuticals, Matrix-assisted laser desorption/ionization-imaging mass spectrometry (MALDI-IMS), Sodium lauryl sulfate, Lipids

Introduction

Healthy skin forms a barrier with the epidermis contributes to the defense mechanism against infection from the environment, and controls water transpiration. The epidermis is composed of a basal layer, a prickle cell layer, and a horny zone. Horny zone can be divided into three layers; horny layer, clear layer and granular layer. Notably, lipids such as ceramide in the horny zone play an important role in skin barrier function. In addition, abnormal balance of lipid composition of the horny zone causes various diseases[1−3].

Surfactants find widespread use as emulsifiers, and as suspending, solubilizing, and stabilizing agents. Due to their unique properties, surfactants are used in the production of many products such as pharmaceuticals, cosmetics, pesticides and detergents. In addition, various detergents are used as skin cleansing products to maintain hygiene. However, surfactants, in particular the hydrophilic detergent sodium lauryl sulfate (SLS), can change permeability in cell membranes in biological systems[4].

* **Corresponding author**
Ikuko Yao
Department of Optical Imaging, Hamamatsu University School of Medicine, 1−20−1 Handayama, Higashi-ku, Hamamatsu, Shizuoka 431−3192, Japan
Tel/Fax: +81−53−435−2092
E-mail: yaoik@hama-med.ac.jp
Received January 28, 2019. Accepted February 27, 2019.
Epub June 11, 2019.
DOI: 10.24508/mms.2019.06.004

SLS is widely used in industrial cleaners and cosmetics, and it lowers the surface tension of aqueous solutions and can dissolve lipid membranes[5]. The main function of a skin cleanser is to remove dirt and grime from the skin surface. However, removal of useful skin lipids results in transient dermatitis and is often followed by a long-lasting hyporeactivity to irritants. Repeated irritation with SLS reduced epidermal barrier function and epidermal water content. In recent years, many studies have investigated skin irritation by SLS[5–7]. However, the specific molecules involved in the mechanism have not been elucidated.

Imaging mass spectrometry (IMS) is a powerful tool that allows simultaneous mapping of many molecules in a tissue section by a single measurement[8]. Our group has developed original IMS equipment in collaboration with Shimadzu Corporation of Japan. The method extends techniques for molecular profiling of different tissue samples, such as the brain[9], liver[10], testis[11], oral tissue[12], whole-eye[13], and retina[14] of rodents, and colon cancer in humans[15] and involves sample preparation, and a nanoparticle-based ionization process in IMS[16]. Notably, MALDI imaging has resulted in many developments for assessing the localization of molecular species in biological samples. Several applications represent the direct entailment of this technology to basic clinical research. In this study, we used IMS to clarify the effect of SLS on the lipoquality of skin which is crucial for its barrier function.

Materials and Methods

Reagents

α-Cyano-4-hydroxycinnamic acid (CHCA) and 2,5-dihydroxybenzoic acid (DHB) were obtained from Bruker Daltonics (Leipzig, Germany). SLS (purity＞99.5%) was purchased from Nacalai Chemicals (Kyoto, Japan) and was used as received.

Animal experiments

We used the foot-pad skin of 8-week-old C57BL/6J male mice from Japan SLC (Shizuoka, Japan). The care and use of laboratory animals was in accordance with the Animal Experiment Regulations of the Hamamatsu University School of Medicine. Mice were anesthetized with chloral hydrate (400 mg/kg, i.p. using a 3.5% aqueous solution) and mounted on a stereotaxic apparatus.

The time schedule of the experiment is shown in Fig. 1A. The mouse foot-pad was treated with 5% SLS for 1 h and dipped in physiological saline for 10 min. Mice were then euthanized and the foot-pads were excised. Physiological saline was applied as a control.

In the experiment showing the extent of trypan blue (TB) infiltration, the foot-pad was washed for 10 min, immersed in 5% aqueous TB solution for 60 min, and finally washed lightly with running water or physiological saline. The tissues for optical microscopy were sectioned to 30 μm thickness at −20°C using a Leica CM1950 cryostat (Leica Microsystems, Wetzlar, Germany). Sections were then placed on a glass slide and embedded in ultraviolet curable resin. The background color of each image obtained by optical microscopy (OLYMPUS, cellSense) was corrected using Adobe Photoshop™ and was then combined. ImageJ (Wayne Rasband, National Institutes of Health, USA) was used for image analysis.

Tissue Preparation for IMS

For IMS, the skin tissues subjected to saline or SLS treatments were directly snap-frozen in liquid nitrogen and sectioned to 15 μm thickness. Continuous frozen sections were thaw-mounted on MAS coated glass slides (Matsunami Glass Industries, Ltd., Osaka, Japan). We used 1.0 mL of CHCA solution (37.8 mg/mL in 60% acetonitrile containing 0.1% TFA) as the matrix to detect SLS. The matrix solution was uniformly sprayed on the tissue surface using a 0.2-mm nozzle-caliber air brush (Procon Boy FWA Platinum; Mr. Hobby, Tokyo, Japan). We used 1.0 mL of DHB solution (50 mg/mL in 50% methanol) as a matrix for lipid detection, by spraying on sections with an air-brush (Procon Boy FWA platinum; Mr. Hobby, Tokyo).

MALDI-IMS

IMS experiments were performed in the positive ionization mode and negative ionization mode using MS-IT-TOF (Mass microscope prototype; Shimadzu Corporation, Kyoto, Japan) in the linear positive and negative modes. The Nd:YAG laser at 355 nm was used at 25% energy and 1000 Hz repetition rate. The interval between data points was 10 μm, sufficient to cover the entire section. Mass spectra were obtained with a scanning mass range of 250 to 300 Da for detecting SLS and with a range of 600 to 910 Da for detecting lipids with a mass resolution of 10,000. Images of skin sections were acquired using the Mass microscope prior to LDI. Data were analyzed using Imaging MS Solution software (ver.1.01.02, Shimadzu) and IMAGERE-

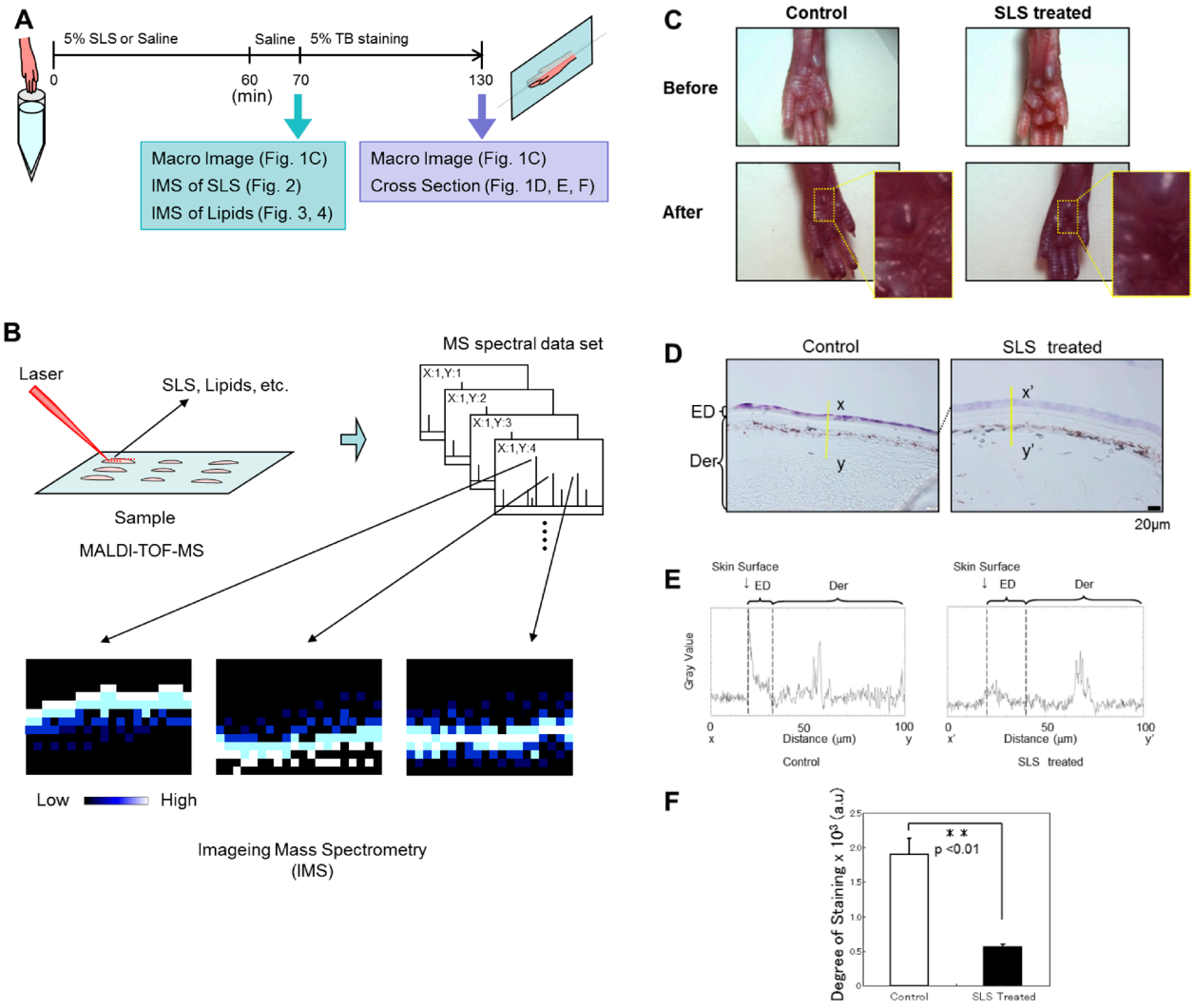

Fig. 1. Experimental design and changes in mouse foot-pads after SLS treatment.

A: Time schedule of the TB immersion experiment. Mouse hind feet were immersed in 5% SLS aqueous solution for 60 min and then washed with physiological saline for 10 min. These samples were used for IMS. To evaluate TB penetration, mouse feet subjected to SLS or control treatment were further immersed in 5% TB for 60 min, followed by sectioning. B: Workflow of imaging mass spectrometry. Multiple sections were sliced using a cryostat and were placed on conductive material. The ion image for specific signals was reconstructed from the obtained spectra. C: Optical images of swollen mouse foot-pads immersed in 5% SLS for 60 min. D: Cross-section optical images of control (left) and SLS-treated (right) mouse foot-pads stained with TB. E: Gray scale intensity of color in the yellow line x–y and x′–y′ indicating histological differences in the sites stained with TB. Arrows indicate the position of the skin surface. The vicinity of the boundary between the surface, epidermis, and dermis is indicated by a dotted line. Scale bar represents 20 μm. F: The degree of staining of the skin cross section was estimated by the integrated value of TB intensity in Fig. 1E. SLS, sodium lauryl sulfate; TB, trypan blue; ED, epidermis; Der, Dermis.

VEAL™ MS software. The experimental design is shown in Fig. 1B.

MS/MS analysis

In order to obtain sufficient signals, one skin sample was used for each measurement. The molecular weight range for the ion trapping was 1.0 Da around the *m/z* of each precursor ion. The setting of the IMS analysis was as follows: laser intensity for fragmentation=50; gas level=50; accumulating time=221 ms; repeating number=1; and 10 μm interval between data points. The other settings were the same as those used for the MS analysis of precursor ions. Mass spectra were obtained with a scanning mass range between 50 and 300 Da with a mass resolution of 10,000.

Statistical analysis

A Student's *t*-test was used for comparison between groups. All data are presented as mean±SEM of the num-

ber of biological replicates (noted in the figure legends).

Results and Discussion

Effect of SLS on skin surface histology

Here, we histologically evaluated the effect of SLS on skin surface. Our results show that SLS caused swelling of mouse foot-pad, as shown in Fig. 1C−F, but the structure of the skin surface was maintained. The images of the foot-pad of mice treated with SLS or saline are shown in Fig. 1C. Strong swelling was observed in the foot-pad of mice treated with SLS than in mice treated with saline.

Subsequently, the extent of TB staining and invasion was histologically measured to observe the extent of damage of the swelling in the foot-pad. The experimental procedure is shown in Fig. 1A. In appearance, (Fig. 1C below), foot-pads of mice treated with SLS were less stained than those of mice treated with saline. We obtained an optical image to observe the microstructure of the foot-pads, and the image was analyzed to evaluate the extent of TB staining and invasion. Cross-sectional images were corrected in Photoshop (Adobe), converted to grayscale, and a graph was obtained by digitizing the gray value in the line connecting points x to y, as shown in Fig. 1D, using Image J software, the results are shown to the left of Fig. 1E. Swelling of the foot-pad of mice treated with SLS was also observed in the optical images. However, noticeable layer structure damage by invasion of TB was not observed in the foot-pad of mice treated with SLS as well as treated with saline. The foot-pad of mice treated with SLS had a lower gray value in the ED layer than in the foot-pad of mice treated with saline. We randomly selected five points and created a similar graph. We confirmed that the result is reproduced.

In addition, this experiment was performed for three skin samples, and the sum of the gray values up to the epidermis was averaged and shown in Fig. 1F. The total gray value was significantly lower for the foot-pads of mice treated with SLS than that for foot-pads of mice treated with saline.

Normal skin has a moisture content of 20−30% and its lamellar structure is stabilized. However, it is suggested that the foot-pad of mide treated with SLS swelled more than that of mice treated with saline because of SLS infiltration, despite no noticeable damage in the layer structure. Furthermore, the fact implies that SLS infiltration in the locations where it occurred caused an increase in water permeability and swelling.

Mass microscope detected SLS signal

In a previous report, repeated exposure to surfactants such as SLS was shown to cause skin function to fail[6]. We assume that SLS infiltrates the skin surface. IMS is useful for directly detecting a target substance without requiring a label. Therefore, we tried to detect SLS on the skin surface using IMS.

Saline and SLS solution were dropped on a mouse tissue section, MS spectra are shown in Fig. 2A (saline), and 2B (SLS). In the region where SLS was dropped, a peak was obtained at *m/z* 265.15. To confirm the signal of *m/z* 265.15 was derived from SLS, we performed MS/MS measurement of the target substance and compared the peaks obtained by fragmentation form standard. From the results in Fig. 2C, a strong peak was observed at *m/z* 96.96, which was considered to be fragmented and was detected in the portion indicated by the arrow in the SLS structural formula shown in Fig. 2C. These results suggested that the *m/z* 265.15 is a peak derived from SLS.

SLS infiltrated into the skin of the mouse foot-pad

Previous experiments revealed that SLS swells the skin of the mouse foot-pad. The result implied that SLS infiltrated into the skin of the mouse foot-pad. In addition, we proved detection of SLS in IMS. Here, we investigated the spectrum of SLS in mice foot-pad treated with SLS using IMS (Fig. 2D, E).

To compare the extent of infiltration of SLS, we divided the skin into stratum corneum (SC), stratum lucidum (SL), stratum granulosum (SG), stratum basale (SB), and dermis regions. The yellow dotted line shows the position of the skin surface. As shown in Fig. 2A, *m/z* 265.15 was observed at a high intensity on the skin surface of the foot-pad of mice treated with SLS as indicated by the dotted line and was found to reach the dermis. We evaluated these imaging results using spectral intensities in each layer of the skin. The intensities in the range selected from the image processing software were compared and the result is shown in Fig. 2E. In the foot-pad of mice treated with SLS, a strong intensity was obtained in the vicinity of the stratum corneum, and a stronger intensity was shown closer to the surface. In the foot-pad of the mice treated with saline, such spectra were obtained in neither the epidermis nor the dermis. In addition, the existence of *m/z* 265.15 was also confirmed on the slide glass. However, this may be because of the SLS dissolved with acetonitrile attached to the surface

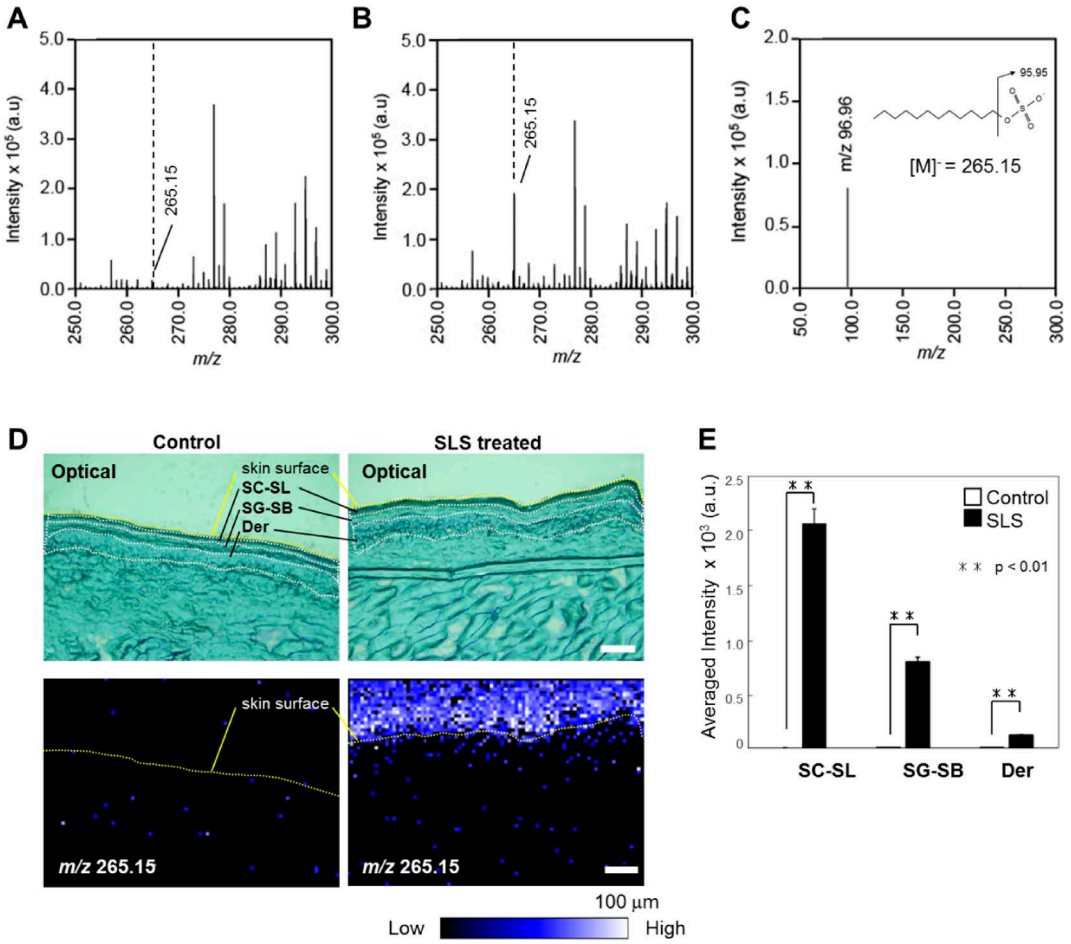

Fig. 2. Detection of sodium lauryl sulfate on the surface of mouse food pad by Mass Microscope.
A: Mass spectrum of a region where saline was dropped on a mouse tissue section as a control. B: Mass spectrum of a region where 5% SLS was dropped. A peak derived from SLS was confirmed at *m/z* 265.15. C: MS/MS result of *m/z* 265.15 as a precursor ion after dropping SLS standard along with matrix solution onto the untreated tissue section. The obtained spectrum showed a peak at *m/z* 96.96 confirming the presence of SLS. D: Imaging of SLS detected as the ion at *m/z* 265.15 in the surface of mouse food pad. The yellow dotted line shows the position of the skin surface. Scale bar represents 100 μm. E: The average signal intensities of the ion at *m/z* 265.15 in the skin treated with or without SLS. SLS, sodium lauryl sulfate; SC−SL, stratum corneum−stratum lucidum; SG−SB, stratum granulosum−stratum basale; Der, Dermis.

of the glass slide during atomization of the matrix at the time of sample preparation. As the visualized data show the respective positional information and spectrum intensity, it is possible to confirm the existence of the target substance in each organization and to compare them by using the software by selecting an arbitrary area of the sample. In the results in Fig. 2B, the signal intensity decreased gradually from the upper layer to the lower layer of the skin of the SLS. Therefore, this result shows the degree of infiltration of SLS into the skin of the foot-pad of mice treated with SLS.

SLS-induced changes skin lipoquality, principally affecting sphingomyelin

Here, we demonstrated the effect of SLS on the distribution of various kinds of lipid molecular species on skin of the mouse foot-pad via IMS. We obtained six types of images of locations where lipids were considered to be present of the mouse foot-pads treated with SLS and saline (Fig. 3). We show that the peaks at *m/z* 608.48, *m/z* 769.58, *m/z* 796.55, *m/z* 817.71, *m/z* 844.55, and *m/z* 894.62 correspond to lyso-phosphatidylcholine (LysoPC) (24:0), sphingomyelin (SM) (d18:1/18:0), phosphatidylcholine (PC) (C16:0/C18:2), SM (d18:0/24:0), PC (C16:0/C22:6), and glucosylcermide (GlcCer) (d18:1/C26:0h) (t18:1/C26:1). Notably, SM (d18:1/18:0), PC (C16:0/C18:2), PC (C16:0/

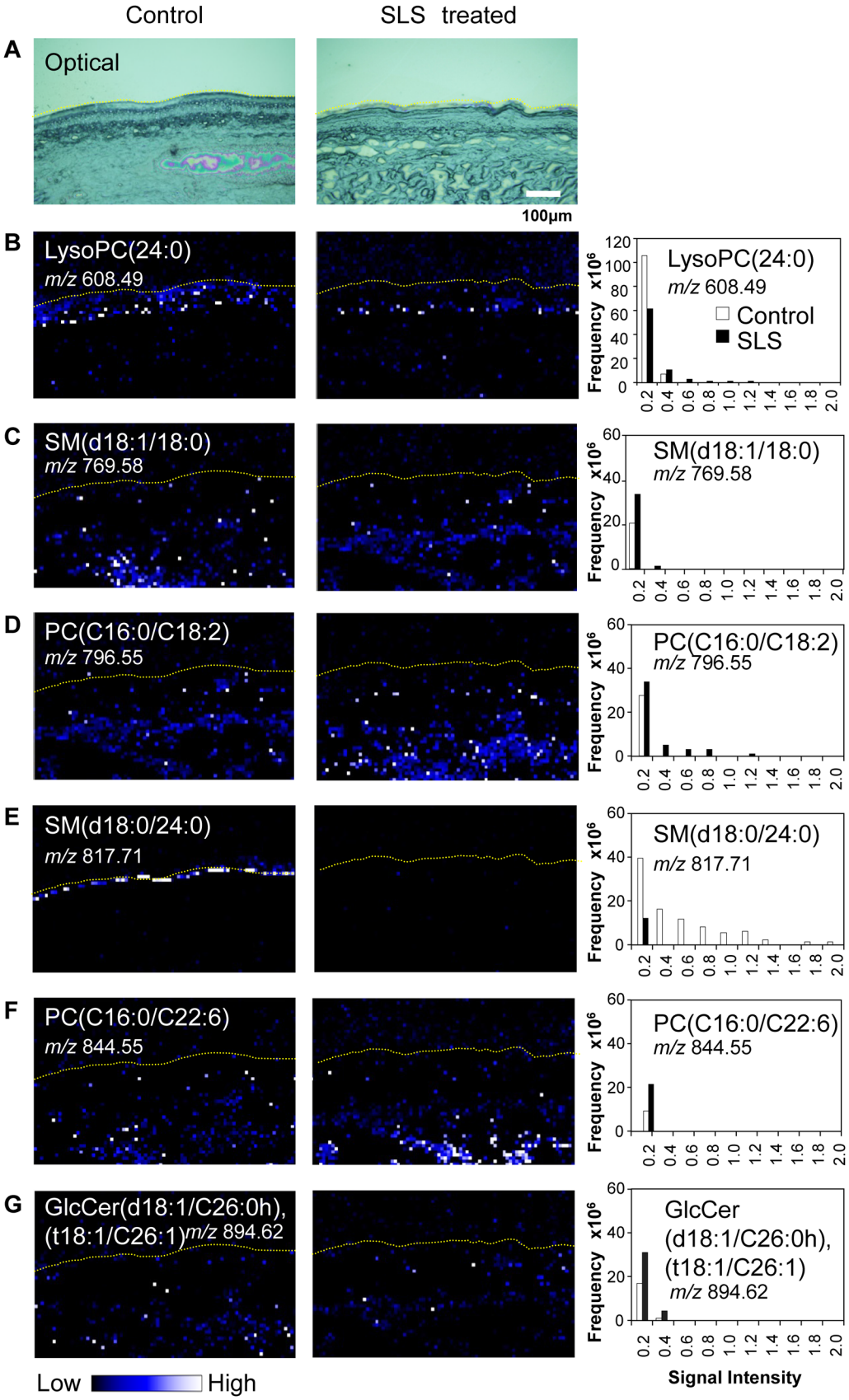

Fig. 3. Specific lipid reduction in the mouse foot-pad skin after SLS application.
A: Optical cross-sectional image of mouse foot-pad skin. The yellow dotted line shows the skin surface. B–G: Mass images of ions at indicated values which correspond to lipids. Histograms show the distribution of their intensity. Scale bar represents 100 μm.

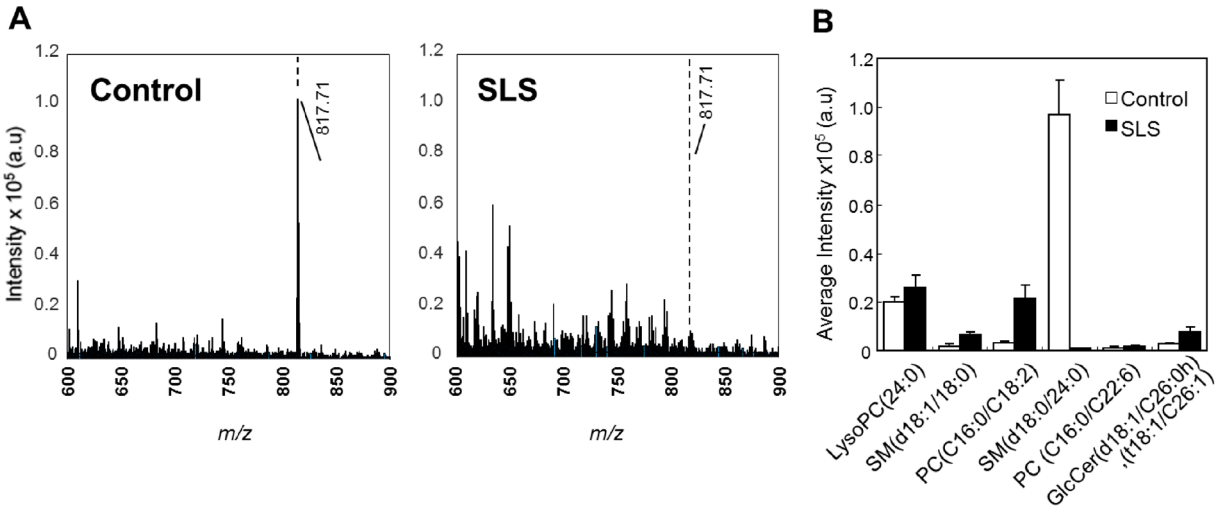

Fig. 4. Disappearance of SM (d18:0/24:0) signal at *m/z* 817.17 from the mouse foot-pad skin surface after SLS application.
A: Averaged mass spectrum in the ROI of the Control or SLS applied skin. B: Comparison of the intensities of respective peaks. White bars indicate Control; black bars represent SLS applied skin.

C22:6), and GlcCer (d18:1/C26:0h) (t18:1/C26:1) have been previously reported to be expressed on the skin of the mouse foot-pad[17]. These four lipid molecular species were located deep in the skin and did not change in the mouse foot-pad treated with SLS compared to the those treated with saline. Hence, this results suggested that single treatment of SLS did not affect lipids in the deep areas of the skin.

In contrast, as shown in Fig. 3E, SM (d18:0/24:0) was located on the surface of the skin of mouse foot-pads treated and decreased in the mouse foot-pads treated with SLS compared to those treated with saline. Fig. 4 shows the histogram of the abundance ratio of these substances in the epidermal surrounding area. SM (d18:0/24:0) had a lower signal intensity in the foot-pads of mice treated with SLS compared to treated with saline. Furthermore, statistical analysis of these data showed that the intensity of SM (d18:0/24:0) was significantly reduced in the mice foot-pad treated with SLS compared with those of mice treated with saline.

These results suggest the effect of SLS on lipids, especially the effect of SM (d18:0/24:0) extraction. SM (d18:0/24:0) exists in the cell membrane at high concentrations. However, the role of SM (d18:0/24:0) in maintaining the barrier function of the skin has not yet been reported.

SLS changed the lipid composition in the epidermis of mouse foot-pad, although the foot-pads were only treated once. Therefore, it is suggested that the removal effect of SLS on lipids may promote skin dysfunction under repetitive SLS treatment. In this study, we suggest the possibility that a change in SM (d18:0/24:0) on the surface is important for skin barrier function.

Conclusion

In this study, using IMS, we demonstrated that SLS penetrates the skin and alters the lipid composition of the skin surface. We found that the lipid composition in the deep parts of the skin does not change. A single treatment of SLS mainly changes the lipid composition on the surface of the skin. Therefore, it is suggested that skin dysfunction due to repeated administration of SLS involves a change in skin lipid composition. Furthermore, various surfactants as well as SLS can cause removal of lipids. Our study proposes reasons to pay attention to the handling of daily surfactants.

Acknowledgements

This study was financially supported by JSPS KAKENHI Grant-in-Aid for Scientific Research Grant Numbers 26460388, 16KT0134 to I.Y, JP15H05898B1 to M. S., by Imaging Platform supported by MEXT, Japan, and by AMED Grant Number JP18gm0910004. The authors also thank the staff members of International Mass Imaging Center and the Advanced Research Facilities and Services, Preeminent Medical Photonics Education and Research Center (Hamamatsu University School of Medicine, Japan) for providing advices and technical assistance.

References

1) Oji V, Tadini G, Akiyama M, Blanchet Bardon C, Bodemer C, et al: Revised nomenclature and classification of inherited ichthyoses: Results of the First Ichthyosis Consensus Conference in Sorèze 2009. *J Am Acad Dermatol* 63(4): 607−641, 2010.
2) Hara J, Higuchi K, Okamoto R, Kawashima M, Imokawa G: High-expression of sphingomyelin deacylase is an important determinant of ceramide deficiency leading to barrier disruption in atopic dermatitis. *J Invest Dermatol* 115(3): 406−413, 2000.
3) Imokawa G, Abe A, Jin K, Higaki Y, Kawashima M, et al: Decreased level of ceramides in stratum corneum of atopic dermatitis: An etiologic factor in atopic dry skin? *J Invest Dermatol* 96(4): 523−526, 1991.
4) Schott H: Surfactant systems: Their chemistry, pharmacy and biology, in Attwood D, Florence AT (eds): Chapman & Hall, London EC4P 4EE, United Kingdom. 1983. 794 pp. *J Pharm Sci* 74(10): 1140−1141, 1985.
5) Okuda M, Yoshiike T, Ogawa H: Detergent-induced epidermal barrier dysfunction and its prevention. *J Dermatol Sci* 30(3): 173−179, 2002.
6) Schliemann S, Schmidt C, Elsner P: Tandem repeated application of organic solvents and sodium lauryl sulphate enhances cumulative skin irritation. *Skin Pharmacol Physiol* 27(3): 158−163, 2014.
7) Heinemann C, Paschold C, Fluhr J, Wigger-Alberti W, Schliemann-Willers S, et al: Induction of a hardening phenomenon by repeated application of SLS: Analysis of lipid changes in the stratum corneum. *Acta Derm Venereol* 85(4): 290−295, 2005.
8) Khatib-Shahidi S, Andersson M, Herman JL, Gillespie TA, Caprioli RM: Direct molecular analysis of whole-body animal tissue sections by imaging MALDI mass spectrometry. *Anal Chem* 78(18): 6448−6456, 2006.
9) Shimma S, Sugiura Y, Hayasaka T, Zaima N, Matsumoto M, et al: Mass imaging and identification of biomolecules with MALDI-QIT-TOF-based system. *Anal Chem* 80(3): 878−885, 2008.
10) Zaima N, Matsuyama Y, Setou M: Principal component analysis of direct matrix-assisted laser desorption/ionization mass spectrometric data related to metabolites of fatty liver. *J Oleo Sci* 58(5): 267−273, 2009.
11) Goto-Inoue N, Hayasaka T, Zaima N, Setou M: The specific localization of seminolipid molecular species on mouse testis during testicular maturation revealed by imaging mass spectrometry. *Glycobiology* 19(9): 950−957, 2009.
12) Miyagi M, Fukano H, Atsumi R, Suzuki H, Setou M, et al: Distinct spatial localization of three types of phosphatidyl choline in rat buccal mucosa identified by matrix-assisted laser desorption/ionization imaging mass spectrometry. *Medical Mass Spectrometry* 1(1): 2−9, 2017.
13) Mori N, Mochizuki T, Yamazaki F, Takei S, Mano H, et al: MALDI imaging mass spectrometry revealed atropine distribution in the ocular tissues and its transit from anterior to posterior regions in the whole-eye of rabbit after topical administration. *PLoS ONE* 14(1): e0211376, 2019.
14) Hayasaka T, Goto-Inoue N, Sugiura Y, Zaima N, Nakanishi H, et al: Matrix-assisted laser desorption/ionization quadrupole ion trap time-of-flight (MALDI-QIT-TOF)-based imaging mass spectrometry reveals a layered distribution of phospholipid molecular species in the mouse retina. *Rapid Commun Mass Spectrom* 22(21): 3415−3426, 2008.
15) Shimma S, Sugiura Y, Hayasaka T, Hoshikawa Y, Noda T, et al: MALDI-based imaging mass spectrometry revealed abnormal distribution of phospholipids in colon cancer liver metastasis. *J Chromatogr B Analyt Technol Biomed Life Sci* 855(1): 98−103, 2007.
16) Goto-Inoue N, Hayasaka T, Sugiura Y, Taki T, Li YT, et al: High-sensitivity analysis of glycosphingolipids by matrix-assisted laser desorption/ionization quadrupole ion trap time-of-flight imaging mass spectrometry on transfer membranes. *J Chromatogr B Analyt Technol Biomed Life Sci* 870(1): 74−83, 2008.
17) Goto-Inoue N, Hayasaka T, Zaima N, Nakajima K, Holleran WM, et al: Imaging mass spectrometry visualizes ceramides and the pathogenesis of dorfman-chanarin syndrome due to ceramide metabolic abnormality in the skin. *PLoS ONE* 7(11): e49519, 2012.